

BURNOUT OF HIGH-TEMPERATURE PRODUCTS OF  
INCOMPLETE COMBUSTION IN A SUPERSONIC  
STREAM WITH SECONDARY INJECTION OF OXIDIZER

Z. G. Shaikhutdinov, A. M. Rusak,  
V. M. Klevanskii, I. S. Saburov,  
and L. F. Shaikhinurova

UDC 533.6:536.46

Results are discussed of an experimental study concerning the burnout of products of incomplete combustion in a supersonic stream by means of secondary injection of oxidizers  $\text{HNO}_3$  or  $\text{N}_2\text{O}_4$ .

Products of incomplete combustion are burned out in a supersonic stream by means of secondary injection of oxidizer, in order to improve the efficiency of drive systems. Conclusions drawn from an analysis of this problem are certainly of interest in a broader scope, inasmuch as the basic aerothermochemical processes of burnout are very similar to processes involved in the design of supersonic combustion systems in general [1].

The authors present here the results of an experimental study concerning the rate and the completeness of combustion in a supersonic stream of products of incomplete combustion with secondary injection of nitrogen compounds  $\text{HNO}_3$  or  $\text{N}_2\text{O}_4$  as oxidizers; also described are the essential features of the test apparatus and the test procedure.

A direct study of burnout processes (chemical analysis and thermometry) in high-temperature supersonic gas streams is rather difficult. The feasibility of obtaining reliable data in this way is also questionable: the stream is very nonhomogeneous and, therefore, gas samples and temperature readings must be taken over the entire cross section, which is not very realistic; the chemical reactions proceed at high rates and this makes the sampling and the conditioning of samples extremely difficult.

The procedure followed in this study made it possible to avoid these difficulties. The rate and the extent of heat generation during burnout was calculated from the change in static pressure which had been measured along the reaction zone [2].

The test apparatus consisted of a gas generator with a special-shape supersonic nozzle, an oxidizer injector assembly with a cylindrical tube attachment, a fluid supply system, and measuring instruments. The basic active components are shown schematically in Fig. 1. Separately shown is the system of oxidizer injection into the supersonic stream: (I) three jet nozzles  $d_j = 0.003$  m in diameter around the circumference of a tube  $d = 0.077$  m in diameter and projecting 0.015 m into the stream for the first test series, and (II) twelve jet nozzles  $d_j = 0.0015$  m projecting into the stream to various depths (three 0.02 m deep, three 0.01 m deep, and six flush with the inside surface of the tube). These arrangements were designed for producing different qualities of carburetion.

For secondary oxidizers we used a 98% solution of nitric acid  $\text{HNO}_3$  and nitrogen tetroxide  $\text{N}_2\text{O}_4$ . The amount of oxidizer injection was varied from test to test over the range  $G_j = 0.2$ -0.9 kg/sec.

Products of incomplete fuel combustion, containing  $g_{\text{H}_2} = 0.0128$  hydrogen and  $g_{\text{CO}} = 0.217$  carbon monoxide, with an  $\alpha = 0.67$  excess oxidizer ratio, were flowing in the mainstream at a rate  $G = 4$ -5 kg/sec. The stagnation parameters were  $T^* = 3000$ -3200°K and  $p^* = 58.8$ -78.4 bars. With nozzle and tube dimensions

---

Translated from *Inzhenerno-Fizicheskii Zhurnal*, Vol. 25, No. 2, pp. 197-203, August, 1973. Original article submitted February 15, 1972.

© 1975 Plenum Publishing Corporation, 227 West 17th Street, New York, N.Y. 10011. No part of this publication may be reproduced, stored in a retrieval system, or transmitted, in any form or by any means, electronic, mechanical, photocopying, microfilming, recording or otherwise, without written permission of the publisher. A copy of this article is available from the publisher for \$15.00.

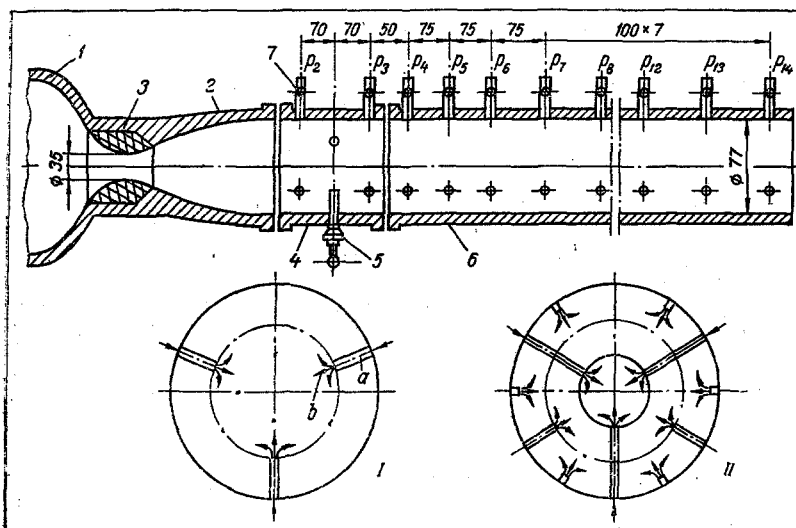


Fig. 1. Schematic diagram of the active portion of the test apparatus: 1) gas generator; 2) special-shape supersonic nozzle; 3) refractory insert; 4) injector assembly; 5) injector set with jet nozzles; 6) cylindrical tube; 7) collector of pressure samples; I, II) schematic diagrams of oxidizer injection systems: a) injection nozzle; b) oxidizer flow diagram.

as shown in Fig. 1, the Mach number and the Reynolds number in the active zone were as high as 2.78 and  $10^6$  respectively.

In our tests we measured the pressure inside the gas generator ( $p_1$ ) with the aid of model ÉDD potentiometer probes, the static-pressure profile ( $p_2$ – $p_{14}$ ) along the tube, and the flow rate of injected oxidizer (with a model DP-10 flow meter). All signals from the instrument transducers were recorded on a model N-700 oscillograph.

Since the channel components and their parts operated under heavy heat loads, the tests had been designed for a minimum necessary duration ( $\tau \approx 2.5$  sec) and a sleeve of a refractive alloy was inserted inside the nozzle at the critical section.

The injection of oxidizer was synchronized with the startup of the apparatus and was discontinued 1.0–1.1 sec later. This made it possible to improve the precision of the test results: the transient conditions in the gas generator ( $T^*$ ,  $p^*$ ) during the period between injection and subsequent operation without injection ( $\tau \approx 0.5$  sec) were maintained almost constant and the pressure jumps recorded on oscillograms were due only to the effects of injection and associated processes: atomization, evaporation, mixing, and burning of the secondary oxidizer.

The test results obtained directly were the static-pressure profiles along the tube shown in Fig. 2. On the same diagram appear also static-pressure profiles along the tube in the absence of any flow perturbations, and during injection of water as a neutral liquid. From the latter we calculated the friction coefficient in the tube, and subsequently developed a method by which the acceleration and the evaporation of liquid under given conditions could be taken into account.

A direct analysis of pressure variations along the tube during injection of liquid reactants will not yield the quantitative characteristics of the processes occurring at that time. However, very interesting conclusions can be drawn from it.

Thus, injection of  $N_2O_4$  causes an appreciably larger increase in static pressure inside the tube than injection of  $HNO_3$ . Since the heat of  $N_2O_4$  evaporation is close to that of  $HNO_3$  evaporation (414 and 610 kJ/kg respectively), hence such a difference between the effects of their injection can be explained only by their different heat generation capability.

The main portion of heat is generated within a small segment of the "combustion chamber," 0.2–0.4 m from the injection zone. Quite noteworthy is the pressure "dip" along some tube segment, probably a result of endothermal processes occurring there.

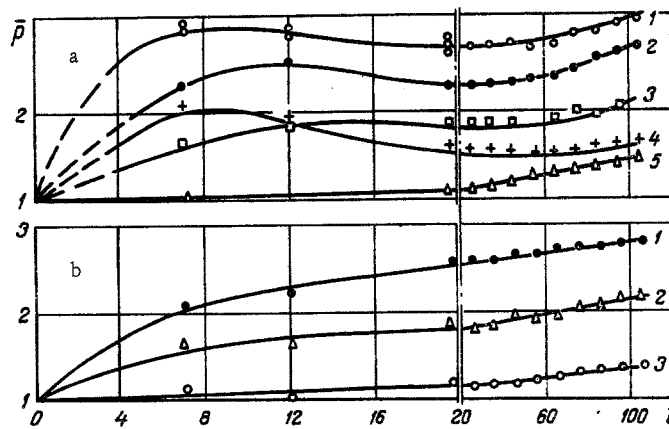


Fig. 2. Static-pressure profile ( $\bar{p} = p/p_\infty$ ) along the tube ( $l$ , cm) with oxidizer injection; a) according to scheme I: 1)  $N_2O_4$   $\bar{G}_j = 0.22$ ; 2)  $N_2O_4$   $\bar{G}_j = 0.16$ ; 3)  $HNO_3$   $\bar{G}_j = 0.20$ ; 4) water injection  $\bar{G}_j = 0.4$ ; 5) pressure in tube without injection; b) according to scheme II: 1)  $N_2O_4$   $\bar{G}_j = 0.02$ ; 2)  $N_2O_4$   $\bar{G}_j = 0.05$ ; 3) pressure in tube without injection.

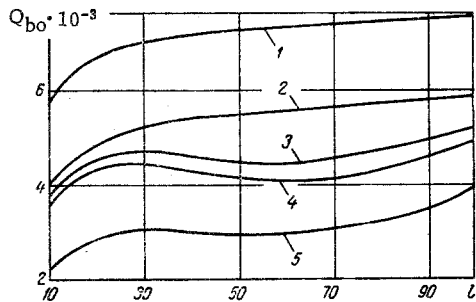


Fig. 3. Calculated heat generation profile ( $Q_{bo}$ , kJ/kg) along the tube ( $l$ , cm) due to burnout with injection of secondary oxidizer: 1)  $N_2O_4$ ,  $\bar{G}_j = 0.05$ ; 2)  $N_2O_4$ ,  $\bar{G}_j = 0.12$ ; 3)  $N_2O_4$ ,  $\bar{G}_j = 0.16$ ; 4)  $N_2O_4$ ,  $\bar{G}_j = 0.22$ ; 5)  $HNO_3$ ,  $\bar{G}_j = 0.2$ .

Burnout seems more efficient with oxidizers injected through the 12-nozzle system. In this case the rate of heat generation increases monotonically along the channel without "dips" as in the case of injection through the 3-nozzle system.

Data on the variation in static pressure have been evaluated with the aid of a computer by an improved version of the method in [2]. Correction factors were introduced to account for heat generation, for qualitative effects of shock waves occurring ahead of the injection zone, and for nonuniformities of acceleration, evaporation, and burnout processes across a tube section. The results of this evaluation are shown in Fig. 3 in terms of heat generation (less the heat of oxidizer evaporation) as a function of the distance along the tube, for various values of the relative oxidizer flow rate.

An analysis of these graphs fully confirms what has been said earlier concerning the qualitative pattern of the burnout processes in the tube. It is to be noted, however, that the burnout efficiency is largely affected by the relative injection rate of oxidizers.

The maximum heat generation in our tests was  $Q_{bo} \approx 7310$  kJ/kg. This value corresponded to an injection of  $N_2O_4$  at a relative rate  $\bar{G}_j = 0.05$  through the 12-nozzle system. With  $N_2O_4$  injection at  $\bar{G}_j = 0.22$  through the 3-nozzle system,  $Q_{bo} \approx 5230$  kJ/kg. For  $HNO_3$  under these conditions,  $Q_{bo} \approx 3560$  kJ/kg.

It is worthwhile to analyze these data from the standpoint of the physical aspect of processes occurring in the tube during injection of secondary oxidizers.

The flow rates of secondary oxidizers are constrained by the requirement of producing a "combustible mixture" throughout the burnout chamber with a negative oxygen balance ( $\alpha < 1$ ). The reaction between an oxidizer and the products of incomplete combustion in the mainstream involves chemical decompositions:



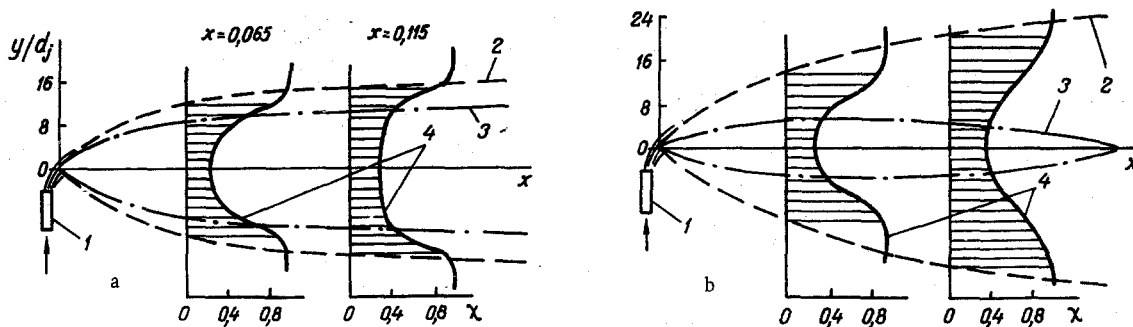


Fig. 4. Mixing profile during water injection into a supersonic gas stream: 1) jet nozzles; 2) outer edge of spray jet; 3) edge of jet core; 4) gas concentration profile along the jet; test conditions: a)  $d_j = 3.12$  mm,  $Ma_\infty = 2.4$ ,  $T_\infty^* = 500^\circ\text{K}$ ,  $p_\infty = 0.4$  bar,  $G_j = 0.525$  kg/sec; b)  $d_j = 1.5$  mm,  $Ma_\infty = 2.4$ ,  $T_\infty^* = 500^\circ\text{K}$ ,  $p_\infty = 0.4$  bar,  $G_j = 0.140$  kg/sec; distance  $x$  (m).

and the net burnout reactions:



which determine the burnout heat  $Q_{bo}$  generated in the tests. Theoretically, many other chemical reactions may occur here, but they are of no significance to our subsequent analysis.

If it is assumed that the amount of  $\text{H}_2$  and  $\text{CO}_2$  units entering the reaction is subject to the condition balance during combustion, then an analysis of reactions (1)-(8) will yield the maximum values of specific heat generation during burnout:  $Q_{bo}^{\max} \approx 11,500$  kJ/kg for  $\text{N}_2\text{O}_4$  and  $Q_{bo}^{\max} \approx 10,000$  kJ/kg for  $\text{HNO}_3$ . The test values of heat generation correspond to the following burnout efficacies:  $\eta_{\text{N}_2\text{O}_4} \approx 0.45$  with injection system I at  $\bar{G}_j = 0.16-0.22$ ,  $\eta_{\text{N}_2\text{O}_4} \approx 0.63-0.50$  with injection system II at  $\bar{G}_j = 0.05-0.12$ , and  $\eta_{\text{HNO}_3} \approx 0.35$  with injection system I at  $\bar{G}_j = 0.2$ .

The decomposition of  $\text{N}_2\text{O}_4$  into  $\text{NO}$  and  $\text{O}_2$  according to reactions (1) and (2) yields 50% free oxygen. A heat generation  $Q_{bo} \approx 3720$  kJ/kg ( $\text{N}_2\text{O}_4$ ) is then possible.

The decomposition of  $\text{HNO}_3$  into  $\text{NO}$ ,  $\text{H}_2\text{O}$ , and  $\text{O}_2$  according to reactions (4) and (5) yields free oxygen in an amount equal to 60% of all oxygen contained in the original oxidizer, and the corresponding heat generation is here  $Q_{bo} \approx 4260$  kJ/kg ( $\text{HNO}_3$ ).

During these stages of oxidizer decomposition, the burnout efficacy in terms of heat generation in our tests was  $\eta_{\text{N}_2\text{O}_4} = 1.4$  with injection system I at  $\bar{G}_j = 0.16-0.22$ ,  $\eta_{\text{N}_2\text{O}_4} = 1.96-1.55$  with injection system II at  $\bar{G}_j = 0.05-0.12$ , and  $\eta_{\text{HNO}_3} = 0.83$  with injection system I at  $\bar{G}_j = 0.20$ .

Assuming burnout to be limited by the oxygen "production" in reactions (2)-(6), and analyzing the efficacy of heat generation, we may conclude that, with the optimum carburation in our tests (low-rate injection through the 12-nozzle system), there was not sufficient time in the experimental "reaction chamber" for a complete decomposition of the oxidizers into  $\text{NO}$  and a partial decomposition of  $\text{NO}$ ; in other words, in this case the heat generation was limited by the kinetics of the slowest of all decomposition reactions from  $\text{NO}$  to  $\text{N}_2$  and  $\text{O}_2$ .

Under other conditions in the injection system, the heat generation was even less efficacious, and in some cases did not even reach a level which it should have with the oxygen produced during the first and fastest stages of oxidizer decomposition alone. This latter circumstance was certainly due to an inadequate carburation.

The flow pattern in a water jet injected into a supersonic gas stream during special tests is shown in Fig. 4. The concentration field here was calculated from temperature readings over cross sections of the interacting stream and jet.

According to the diagram, the spray jet of liquid in a supersonic stream consists of two distinct zones: the core with a low gas concentration

$$\chi = \frac{G_g}{G_g + G_j} \approx 0.30 - 0.45$$

and a turbulent mixing zone with the gas concentration varying from between 0.45 and 0.50 at the inner edge to 1.0 at the outer edge.

An analysis shows that such a jet structure can be retained in a supersonic stream through quite a long distance, when coming from injection nozzles  $d_j = 0.003$  m in diameter, but is "sucked in" much faster when coming from injection nozzles  $d_j = 0.0015$  mm in diameter.

The amounts of gas contained in the jet core are sufficient for fast evaporation and decomposition of the oxidizer ( $T^* \approx 800-1500^\circ\text{K}$ ), but not sufficient for completing the burnout processes. This explains the different efficacies of burnout during injection in our first and second test series.

At a short distance from the injection zone, the processes of evaporation, decomposition, and combustion may initially occur at high rates in both the jet core and in the boundary zone of turbulent mixing. As a consequence, the pressure inside the tube rises fast. Evaporation and decomposition of the oxidizer in the jet core continue at high rates, as if accelerating the stream as a whole. The heat generated by burnout processes does not have time here (under specific conditions) to compensate even for the heat lost on evaporation and decomposition, causing the "dip" noted in the heat generation profile along the tube.

No explicit data are available, so far, which would explain the wide difference between burnout with  $\text{N}_2\text{O}_4$  and with  $\text{HNO}_3$  injection respectively. It has probably to do with the less effective kinetics of  $\text{HNO}_3$  injection, but could also be due to the different properties of these two substances and the consequent differences in their carburetion.

#### NOTATION

Ma	is the Mach number;
Re	is the Reynolds number;
p	is the pressure;
T	is the temperature;
l	is the channel length;
d	is the tube diameter;
x, y	are the space coordinates in the plane of symmetry of the jet;
$Q_{bo}$	is the specific heat of burnout;
$\alpha$	is the excess oxidizer ratio;
$\chi$	is the concentration of the fuel gas in the spray jet;
$\eta$	is the burnout efficacy;
$\bar{G}$	is the mass flow rate (per second);
$\bar{G}$	is the relative flow rate;
$\tau$	is time;
g	is the mass fraction of a component.

#### Subscripts

g	refers to gas;
j	refers to injected liquid;
$\infty$	refers to nozzle throat section;
*	refers to stagnation values of parameters.

#### LITERATURE CITED

1. A. Ferry, P. A. Libby, and V. Zakay, High Temperatures in Aeronautics, Pergamon Press (1963), pp. 55-118.
2. Z. G. Shaikhtudinov and A. M. Rusak, Inzh. Fiz. Zh., 21, No. 5 (1971).